L^2 discretization and complex coordinates in the calculation of bound-free amplitudes in the presence of long-range forces

Bruce R. Johnson
Department of Chemistry, University of Colorado, Boulder, Colorado 80309
and Joint Institute for Laboratory Astrophysics,
University of Colorado and National Bureau of Standards, Boulder, Colorado 80309

William P. Reinhardt*
Molecular Spectroscopy Group, National Bureau of Standards, Washington, D.C. 20234
(Received 4 May 1983)

The formalism of Møller wave operators is shown to provide a stable basis for computation of bound-free transition amplitudes for both short- and long-range potentials without the direct calculation of scattering wave functions. This method, which relies on the techniques of expansion in finite L^2 bases and rotation of the coordinates into the complex plane, is applied to both an exponential potential and one that behaves asymptotically as $-1/r^4$. It is demonstrated that one obtains not only accurate magnitudes of the matrix elements, but accurate phases (i.e., the scattering phase shift) as well. Some relevant theoretical results with regard to the application of wave operators are also presented. Although couched in terms of potential scattering, the procedures are readily extendible to multichannel problems.

I. INTRODUCTION

In the theoretical pursuit of such experimentally important quantities as partial cross sections and angular distributions, it becomes clear that accurate systematic methods for the direct computation of transition amplitudes would prove very valuable. This paper represents a first step towards the development of procedures for calculation of bound-free (e.g., photoabsorption) amplitudes based on the formalism of Møller wave operators.[1-3] Using complex coordinate[4,5] and L^2 discretization[6] techniques, we show that one-body matrix elements of this sort can be obtained for either short- or long-range forces without directly calculating the appropriate continuum wave functions. As examples, both the exponential potential $-\exp(-r)$ and a potential which behaves asymptotically as $-\alpha/r^4$ (representing polarization forces) are investigated in detail. These calculations also provide an opportunity to check some new results, derived below, in the theory of wave operators for central potentials.

Earlier applications of complex coordinates and discrete basis set methods to photoabsorption[7-15] have proven capable of accurately determining the total cross section, that is, the total probability of excitation and ionization into all of the accessible channels. However, it has not been found possible to obtain partial cross sections (or widths) except with techniques requiring explicit enforcement of multichannel boundary conditions.[16-19] The present calculations, in contrast, should be easily extendible to multichannel problems.

It is well known[20-24] that complex coordinate techniques cannot be used in a straightforward way to calculate scattering amplitudes in the presence of long-range potentials (i.e., potentials which are not exponentially bounded). If $\psi_0(k,r)$ is the regular spherical Bessel function for some angular momentum, then the expression for the partial wave T-matrix element,

$$\langle\psi_0|T|\psi_0\rangle=\langle\psi_0|V|\psi_0\rangle + \langle\psi_0|V(E+i\epsilon-H)^{-1}V|\psi_0\rangle\ , \quad (1.1)$$

cannot survive the coordinate rotation $r\rightarrow re^{i\theta}$ since the factor $V(r)\psi_0(k,r)$ then diverges as $r\rightarrow\infty$ unless $V(r)$ decreases exponentially.

However, our interests lie in calculating a bound-free amplitude of the form

$$\langle\Phi_{\text{bound}}|\psi\rangle\ , \quad (1.2)$$

where Φ_{bound} is some square-integrable function. (In photoabsorption contexts, it is the product of a bound eigenfunction of the Hamiltonian and the dipole moment operator.) It is an important point here that the full scattering solutions are not needed in order to calculate such bound-free amplitudes since the integration in the transition matrix element is effectively and smoothly cut off by the presence of the L^2 function. Thus Φ_{bound} provides the required exponential damping of the matrix element and, as far as coordinate rotation is concerned, $V(r)$ may be either short or long range. It turns out that, in the present paper, it is the Coulomb potential (with all its attendant complexities) where the line must be drawn. We require that the interaction potential decays faster than $1/r$ so that the standard theory of Møller operators[2,3] may be used. This also leads us to require that V not be more singular than $1/r^2$ at the origin. Thus, in this first stage of development, a technique is presented which is applicable to computation of channel by channel partial cross sections and angular distributions for photodetachment of negative ions (leaving a neutral atom in the final state). The two-body Coulomb problem is the subject of an upcoming paper.[25]

The fact that we need the continuum wave function only over a finite region of space suggests finite L^2-basis techniques. It is evident that, if the continuum wave function is expanded in a complete square-integrable basis which becomes increasingly diffuse in higher order, then the contributions of the successive basis functions to a damped matrix element as in Eq. (1.2) will drop off after some point in the expansion. This stirs hope for the existence of a convergent variational procedure for the matrix element. In fact, it has been amply demonstrated that diagonalization of the Hamiltonian in this finite basis provides a dependable method for determining the relevant expansion coefficients up to a common overall factor. An eigenvector (unit-normalized) coming out of the matrix diagonalization can be interpreted as a legitimate continuum function (delta-function-normalized) over this restricted region, except for an implicit renormalization. There are some one-body cases where the change in normalization can be pinned down by use of the method of "equivalent quadrature."[6,26–28] A more general and widely applied technique is that of Stieltjes imaging.[29–31]

The theory of Møller wave operators,[1–3] $\Omega^{\pm}$, which seems to have found mostly formal use in the past, provides another possible computational framework for avoiding the problem of unknown normalization. (See, however, Refs. 32 and 33, in which the wave operators are used in the calculation of t-matrix elements.) For the purposes of this paper $\Omega^{\pm}$ are simply regarded as operators which convert free-particle wave functions ψ_0 into continuum functions $\psi^{\pm}$ appropriate to a particular scattering potential:

$$\psi^{\pm}(k,r)=\Omega^{\pm}\psi_0(k,r) \ . \tag{1.3}$$

Inserting this into Eq. (1.2) then yields

$$\langle \Phi_{\text{bound}} \mid \psi^{\pm}(k)\rangle = \langle \Phi_{\text{bound}} \mid \Omega^{\pm} \mid \psi_0(k)\rangle \ . \tag{1.4}$$

In this context $\Omega^{\pm}$ may be couched in terms of the resolvent, for which matrix elements may be obtained to high accuracy through finite-basis techniques,[6,11,29,30] with only a single diagonalization of a (complex) Hamiltonian being required in order to cover a continuous range of the energy. Since the absolute normalization of ψ_0 is a known quantity, that of ψ is built into the calculation. Also, the correct asymptotic behavior of $\psi^{\pm}$ can then be controlled by the choice of ψ_0, a fact which suggests a simple technique for obtaining partial cross sections in a multichannel extension of Eq. (1.4). Furthermore, the use of complex coordinates allows the branch cut(s), implicit in the usual time-independent integral representations of the wave operators, to be rotated away from the real energy axis, and thus the L^2 expansions can be employed directly, yielding a convergent algorithm for evaluation of amplitudes in the $E+i\epsilon$ limit without analytic continuation or extrapolation in the energy or momenta.[34–44]

Wave operators as such are normally applied to free-particle wave functions ψ_0 (spherical Bessel functions in the present case) which are regular at the origin. If, however, the regular function is written as a linear combination of the irregular functions (Hankel functions or spherical waves), it is clear that use of complex coordinates causes one of the irregular functions to increase exponentially at infinity and the other to decrease exponentially. [This is, again, the essential reason why the method cannot be used for long-range scattering amplitude calculations as in Eq. (1.1).] For this reason, we have investigated both theoretically and computationally exactly what happens when the wave operator is applied to one irregular solution at a time. The theoretical results are simple and involve the Jost irregular solutions[2] to the full Schrödinger equation. The computational results focus on the relative numerical stabilities obtained in using the decreasing and increasing exponentials.

Two formally identical, but computationally distinct, forms of the wave operator are investigated. Further, Padé approximants[45] are introduced at a certain stage to be described later. For one form of the wave operator, this is not absolutely necessary, but it does accelerate the convergence for the long-range example. For the other form, the approximants appear to be indispensable. In addition to demonstrating that converged bound-free amplitudes may be obtained using L^2 discretization and complex coordinates, the methods also give well-converged values of the elastic scattering phase shift for the single-channel problems considered here.

Finally, we note that the motivation for developing the present formalism is the hope that it may be extended to the partial cross section for double-electron photoionization of H^-,

$$H^- + \hbar\omega \rightarrow H^+ + e^- + e^- \ . \tag{1.5}$$

This process is the subject of intense interest experimentally[46] and theoretically.[47–52] At present the behavior of the partial photoionization cross section near the three-body breakup threshold is still a matter of debate. Of course, construction of the amplitude for this process is likely to be very difficult, especially near threshold, but the preliminary results here and in the two-body Coulomb problem[25] are at least encouraging.

The order of the paper is as follows. In Sec. II, a brief review is given of the important functions in the theory of single-channel scattering by a central potential. This is followed by the theoretical results of applying the wave operators, not to the physical wave function, but to the irregular ones; proofs are left for the Appendix. Section III is devoted to a description of the numerical calculations, including the use of Padé approximants and different forms of the wave operator. The short-range potential is treated in Sec. IV, followed in Sec. V by the long-range potential. Detailed comparisons are made for the purposes of determining the most accurate routes of calculation. A discussion is then given in Sec. VI.

II. SCATTERING PRELIMINARIES

A. Partial waves and associated functions

For a spherically symmetric potential $V(r)$,[53] the partial wave Hamiltonian H is taken to be

$$H=H_0+V(r) \ , \tag{2.1}$$

where

$$H_0=-\frac{1}{2}\frac{d^2}{dr^2}+\frac{l(l+1)}{2r^2} \tag{2.2}$$

and $V(r)$ is a "reasonable" potential.[2,3,54] (Specifically, we are excluding the Coulomb potential.) The irregular solutions to the Schrödinger equation,

$$(H-\tfrac{1}{2}k^2)f_\pm(k,r)=0 \tag{2.3}$$

(k in general complex), are required to satisfy the asymptotic conditions

$$\lim_{r\to\infty} f_\pm e^{\mp ikr}=1\ . \tag{2.4}$$

The functions $f_\pm(k,r)$ are sometimes called the Jost irregular solutions. From f_+ one can obtain the Jost function in the limit $r=0$,

$$F_+(k)=\lim_{r\to 0}(2l+1)r^l f_+(k,r)\ . \tag{2.5}$$

In the limit that $|k|\to\infty$, this approaches $(2l+1)!!\exp(-il\pi/2)$. For some purposes it is also convenient to define a Jost function which approaches unity at large $|k|$,

$$J_+(k)=\frac{(-ik)^l}{(2l+1)!!}F_+(k)\ . \tag{2.6}$$

This latter function is also known as the Fredholm determinant[2]; for real k, $\arg(J_+)$ is the negative of the potential scattering phase shift.

The regular solution of the Schrödinger equation, $\phi(k,r)$, which obeys the boundary condition

$$\lim_{r\to 0} r^{-l-1}\phi(k,r)=1\ , \tag{2.7}$$

is a linear combination of the two irregular solutions:

$$\phi(k,r)=\frac{1}{2ik}[F_-(k)f_+(k,r)-F_+(k)f_-(k,r)]\ . \tag{2.8}$$

The regular function is related to the physical wave function,[55] $\psi(k,r)$, by a simple proportionality factor,

$$\begin{aligned}\psi(k,r)&=ki^l\phi(k,r)/F_+(k)\\&=\tfrac{1}{2}i^{l+1}[f_-(k,r)-S(k)f_+(k,r)]\ .\end{aligned} \tag{2.9}$$

Here $S(k)$ is the S-matrix element for angular momentum l,

$$S(k)=F_-(k)/F_+(k)\ . \tag{2.10}$$

Note that, for k real, Eqs. (2.6) and (2.9) allow ψ to be cast into the form of a real function times the complex conjugate of the Jost function,

$$\begin{aligned}\psi&=i^l F_-\frac{1}{2i}(f_+/F_+-f_-/F_-)\\&=J_-\frac{1}{2i}(i^{-l}f_+/J_+-i^l f_-/J_-)\ ,\end{aligned} \tag{2.11}$$

and, thus, the argument of the physical wave function is the phase shift (modulo π).

For $V=0$, we have the limits

$$J_\pm(k)\to 1\ , \tag{2.12}$$

$$f_\pm(k,r)\to f_{0\pm}(k,r)=i^{\pm(l+1)}\hat{h}_l^{(1,2)}(kr)\ , \tag{2.13}$$

and

$$\psi(k,r)\to\psi_0(k,r)=\hat{j}_l(kr)\ , \tag{2.14}$$

where spherical Ricatti-Bessel functions have been introduced:

$$\hat{j}_l(x)=(\pi x/2)^{1/2}J_{l+1/2}(x)\ , \tag{2.15}$$

$$\hat{\eta}_l(x)=(\pi x/2)^{1/2}N_{l+1/2}(x)\ , \tag{2.16}$$

and

$$\begin{aligned}\hat{h}_l^{(1,2)}(x)&=(\pi x/2)^{1/2}H^{(1,2)}_{l+1/2}(x)\\&=\hat{j}_l(x)\pm i\hat{\eta}_l(x)\ .\end{aligned} \tag{2.17}$$

The full and free physical wave functions are related by the partial wave Møller operator Ω, whose action on ψ may be put into the alternative forms

$$\psi=\Omega\psi_0=\lim_{\epsilon\to 0} i\epsilon G(K)\psi_0 \tag{2.18a}$$

$$=\lim_{\epsilon\to 0}[1+G(K)V]\psi_0\ . \tag{2.18b}$$

Here G is the resolvent, or Green's operator,

$$G(K)=(\tfrac{1}{2}K^2-H)^{-1}\ , \tag{2.19}$$

and K is related to k (which is hereafter real) by

$$\tfrac{1}{2}K^2=\tfrac{1}{2}k^2+i\epsilon,\quad \mathrm{Im}K>0\ . \tag{2.20}$$

In obtaining Eq. (2.18b), we have used the identity

$$0=(H_0-\tfrac{1}{2}k^2)\psi_0=(H-\tfrac{1}{2}K^2+i\epsilon-V)\psi_0\ . \tag{2.21}$$

Hereafter, we shall simply write $i\epsilon G$ or $1+GV$, *and the limit* $\epsilon\to 0$ *is to be regarded as implicit.*

There is one more function that will be important to have at our disposal, the Green's function. This is the kernel of the Green's operator, and satisfies the inhomogeneous differential equation,

$$(H-\tfrac{1}{2}K^2)G(K;r,r')=-\delta(r-r')\ . \tag{2.22}$$

The Green's function is explicitly given by

$$\begin{aligned}G(K;r,r')&=-\frac{2}{Ki^l}\psi(K,r_<)f_+(K,r_>)\\&=\frac{1}{iK}[f_-(K,r_<)-S(K)f_+(K,r_<)]f_+(K,r_>)\ ,\end{aligned} \tag{2.23}$$

the variables $r_<$ and $r_>$ representing, respectively, the lesser and greater of r and r'.

B. Wave operators and irregular solutions

One crucial point about the equality of Eqs. (2.18a) and (2.18b) is that the physical wave function vanishes at the origin. Later on we shall be interested in the effect of applying the wave operator to one or the other of the irregu-

lar solutions instead of the regular one. It is proven in the Appendix that

$$i\epsilon G f_{0\pm} = (1+GV) f_{0\pm} - i^{-l\pm l} f_+ / J_+ \tag{2.24}$$

which is an inhomogeneous analog of the equation satisfied by ψ_0. The inhomogeneous terms, themselves solutions of the full Schrödinger equation, arise because $f_{0\pm} \propto r^{-l}$ as $r \to 0$ [see Eq. (2.13)]. Note from Eq. (2.14) that the free physical wave function is simply

$$\psi_0 = \frac{1}{2i}(i^{-l} f_{0+} - i^{l} f_{0-}) \tag{2.25}$$

and thus the full physical wave function is

$$\psi = \frac{1}{2i}[i^{-l}(i\epsilon G f_{0+}) - i^{l}(i\epsilon G f_{0-})] \ . \tag{2.26}$$

Therefore, the inhomogeneous terms in Eq. (2.24) cancel, correctly yielding Eq. (2.18b).

It is also proven in the Appendix (the proof is for $l=0$; we conjecture the result for all l) that

$$i\epsilon G f_{0+} = 0 \ , \tag{2.27}$$

$$i\epsilon G f_{0-} = 2i^{-l-1}\psi \ . \tag{2.28}$$

With Eq. (2.24), these immediately imply that

$$(1+GV) f_{0+} = f_+ / J_+ \ , \tag{2.29}$$

$$(1+GV) f_{0-} = 2i^{-l-1}\psi + (-1)^{l+1} f_+ / J_+ \ . \tag{2.30}$$

Thus, in using the $i\epsilon G$ form of the wave operator, only one Hankel function contributes. By way of contrast, both Hankel functions contribute when $1+GV$ is used. This distinction will be of interest when we come to the computations, where both forms of the wave operators are used for independent calculations of photoionization-type amplitudes.

It is a remarkable fact that, although the potential has specifically been assumed to be non-Coulombic, the proofs in the Appendix for Eqs. (2.24), (2.27), and (2.29) in no way depend on this assumption. Thus they all hold for the Coulomb problem. [The corresponding physical, irregular, Jost, and Green's functions are all given in, e.g., Ref. 2, the major difference consisting of the familiar logarithmic modification of the asymptotic conditions in Eq. (2.4).] Equations (2.28) and (2.30) do not carry over. There are analogous equations that hold in the Coulomb case, but they entail an infinite phase factor in the limit that $\epsilon \to 0$. This is connected to the fact that the wave operators for the Coulomb problem are not the same as considered in this paper.

III. COMPLEX COORDINATES AND RESOLVENT APPROXIMATIONS

A. $1+GV$

It is clear from the discussion of wave operators in Sec. II that their use in computations will entail constructing matrix elements of the resolvent (damped by the presence of some L^2 function, of course) for the argument z of the resolvent close to the positive real axis. The combined methods of complex coordinates and finite basis calculations have proven to work extremely well in applications of this sort.

From Eq. (2.18), the full and free physical wave functions are related by

$$\psi = (1+GV)\psi_0 \ . \tag{3.1}$$

Equation (3.1) is projected onto the bra $\langle A \mid$,

$$\langle A \mid \psi \rangle = \langle A \mid \psi_0 \rangle + \langle A \mid GV \mid \psi_0 \rangle \ , \tag{3.2}$$

where $A(r)$ is square integrable and

$$\langle A \mid GV \mid \psi_0 \rangle = \int_0^\infty dr\, A(r)(z-H)^{-1} V(r) \psi_0(k,r) \ , \tag{3.3}$$

$$z = \tfrac{1}{2}k^2 + i\epsilon \ . \tag{3.4}$$

The first term on the right-hand side of Eq. (3.2) should usually be easy to calculate. The other term is subjected to a contour rotation, or rather, an application of the unitary transformation U_θ which scales r by $\exp(i\theta)$:

$$\begin{aligned}\langle A \mid GV \mid \psi_0 \rangle &= \langle A \mid U_\theta^\dagger U_\theta G V U_\theta^\dagger U_\theta \mid \psi_0 \rangle \\ &= \langle A_\theta \mid (z-H_\theta)^{-1} V_\theta \mid \psi_{0\theta} \rangle \\ &= \int_0^\infty dr\, A_\theta(r)(z-H_\theta)^{-1} V_\theta(r) \psi_{0\theta}(k,r) \ .\end{aligned} \tag{3.5}$$

Here the rotated quantities are defined by[56]

$$A_\theta(r) = U_\theta A(r) = e^{i\theta/2} A(re^{i\theta}) \ , \tag{3.6}$$

$$H_\theta = U_\theta H U_\theta^\dagger = H_{0\theta} + V_\theta = e^{-2i\theta} H_0 + V_\theta \ , \tag{3.7}$$

$$V_\theta(r) = U_\theta V(r) U_\theta^\dagger = V(re^{i\theta}) \ , \tag{3.8}$$

$$\begin{aligned}\psi_{0\theta}(k,r) &= U_\theta \psi_0(k,r) = e^{i\theta/2} \psi_0(k, re^{i\theta}) \\ &= e^{i\theta/2} \hat{j}_l(kre^{i\theta}) \ .\end{aligned} \tag{3.9}$$

The utility of the rotation is that, within a finite region of coordinate space, the rotated resolvent (with z real) can be well approximated by

$$\langle r \mid (z-H_\theta)^{-1} \mid r' \rangle \cong \sum_{i=1}^{N} \frac{\chi_{i\theta}(r)\chi_{i\theta}(r')}{z-E_{i\theta}} \ , \tag{3.10}$$

where the wave functions $\chi_{i\theta}(r)$ are complex linear combinations of real orthogonal basis functions. In the present computations we have taken these to be Laguerre functions of order $2l+2$,

$$\chi_{i\theta}(r) = \sum_{n=0}^{N-1} a_{in}(\theta) \Phi_n(r) \ , \tag{3.11}$$

$$\Phi_n(r) = \left[\frac{n!\lambda}{(n+2l+2)!} \right]^{1/2} (\lambda r)^{l+1} L_n^{2l+2}(\lambda r) e^{-\lambda r/2} \ . \tag{3.12}$$

The complex coefficients and energies used here are obtained by numerical diagonalization of the rotated Hamiltonian H_θ. The continuum eigenvalues of the latter fall roughly on the ray at angle $\exp(-2i\theta)$ from the origin of the complex energy plane, and thus ensure that the poles in Eq. (3.10) do not come close to the positive real axis.

This allows the $\epsilon \to 0$ limit to be taken directly by simply setting $z=E=k^2/2$.

Using Eqs. (3.10), (3.11), and the resolution of the identity

$$\sum_{n=0}^{\infty} \Phi_n(r)\Phi_n(r') = \delta(r-r') , \tag{3.13}$$

in the appropriate places in Eq. (3.5), the matrix element involving the resolvent becomes

$$\begin{aligned}\langle A \mid GV \mid \psi_0 \rangle &\cong \sum_{i=1}^{N} \langle A_\theta \mid \chi_{i\theta} \rangle (z-E_{i\theta})^{-1} \langle \chi_{i\theta} \mid V_\theta \mid \psi_{0\theta} \rangle \\ &= \sum_{i=1}^{N} \sum_{n=0}^{N-1} \sum_{n'=0}^{N-1} \langle A_\theta \mid \Phi_n \rangle \langle \Phi_n \mid \chi_{i\theta} \rangle (z-E_{i\theta})^{-1} \langle \chi_{i\theta} \mid \Phi_{n'} \rangle \langle \Phi_{n'} \mid V_\theta \mid \psi_{0\theta} \rangle \\ &= \sum_{i,n,n'} \langle A_\theta \mid \Phi_n \rangle a_{in} (z-E_{i\theta})^{-1} a_{in'} \langle \Phi_{n'} \mid V_\theta \mid \psi_{0\theta} \rangle . \end{aligned} \tag{3.14}$$

As long as the left- and right-hand matrix elements can be computed easily, this provides a convenient approximation procedure for the total matrix element which converges with increasing basis size N.

Although these procedures (and those in Sec. III B) have been phrased in terms of ψ_0, it was expected that the matrix element with f_{0+} would show better convergence because of the exponential damping. Therefore, guided by the theoretical results of Sec. II B, the amplitudes involving $f_{0\pm}$ were also computed for comparison.

B. $G(z-H_0)$

The operator $i\epsilon G$, with its implicit singular limit, provides an unattractive basis for numerical experiments. There is another form of the wave operator, however, which gives rise to a nonsingular approximation scheme similar to that in the last section. Using the identity

$$i\epsilon\psi_0 = (z-H_0)\psi_0 , \tag{3.15}$$

Eq. (2.18) may also be written as

$$\psi = (z-H)^{-1}(z-H_0)\psi_0 . \tag{3.16}$$

Projecting onto $\langle A \mid$ and performing the contour rotation again,

$$\begin{aligned}\langle A \mid \psi \rangle &= \langle A \mid (z-H)^{-1}(z-H_0) \mid \psi_0 \rangle \\ &= \langle A \mid U_\theta^\dagger U_\theta (z-H)^{-1}(z-H_0) U_\theta^\dagger U_\theta \mid \psi_0 \rangle \\ &= \langle A_\theta \mid (z-H_\theta)^{-1}(z-H_{0\theta}) \mid \psi_{0\theta} \rangle . \end{aligned} \tag{3.17}$$

The new operator $z-H_{0\theta}$ can be approximated within the same N-term basis by

$$\langle r \mid (z-H_{0\theta}) \mid r' \rangle \cong \sum_{i=1}^{N} \chi_{i\theta}^{(0)}(r)(z-E_{i\theta}^{(0)})\chi_{i\theta}^{(0)}(r') , \tag{3.18}$$

where the wave functions are, in analogy to Eq. (3.11),

$$\chi_{i\theta}^{(0)}(r) = \sum_{n=0}^{N-1} a_{in}^{(0)} \Phi_n(r) , \tag{3.19}$$

and where the coefficients and eigenvalues come from diagonalization of $H_{0\theta}$. [Note that this is equivalent to diagonalizing H_0 since it differs from $H_{0\theta}$ only by a multiplicative factor of $\exp(-2i\theta)$.] The quantity that is finally computed is then

$$\begin{aligned}\langle A \mid \psi \rangle \cong \sum_{i,i'=1}^{N} \sum_{n,n',n''=0}^{N-1} [&\langle A_\theta \mid \Phi_n \rangle a_{in} (z-E_{i\theta})^{-1} a_{in'} \\ &\times a_{i'n'}^{(0)} (z-E_{i'\theta}^{(0)}) a_{i'n''}^{(0)} \langle \Phi_{n''} \mid \psi_{0\theta} \rangle] . \end{aligned} \tag{3.20}$$

To our knowledge, numerical implementation of an expansion of the type in Eq. (3.20) has not been previously carried out. However, we shall show in Secs. IV and V that, at least with the aid of Padé approximants, it does indeed succeed. Previous work has shown the efficiency of coordinate rotation and discrete basis sums as in Eq. (3.10) in calculating matrix elements of the resolvent $(z-H)^{-1}$. Contour distortion, or analytic continuation, arguments suggest that if H is transformed to H_θ, H_0 ought to be simultaneously replaced by $H_{0\theta}$. There is a related motivation in applying the unitary transformation for coordinate rotation to both operators. It is evident that we want to rotate H in $(z-H)^{-1}$ in order to push the poles away from the positive real energy axis. The rotation of H_0 in $z-H_0$ has the practical, and desirable, effect of rotating unwanted zeros in the total matrix element [Eq. (3.20)] away from this axis.

One further point deserves mention. Comparison of Eqs. (3.14) and (3.20) shows that the $G(z-H_0)$ method involves an additional resolution of the identity than does the $1+GV$ method. This suggests that the latter should be the more accurate.

C. Padé approximants

In an effort to extract as much information as possible from the data for a given basis size, we have also introduced the use of Padé approximants. To see where these come in, note that we may rewrite Eq. (3.14) as

$$\langle A \mid GV \mid \psi_0 \rangle \cong \sum_{n'=0}^{N-1} b_{n'} \langle \Phi_{n'} \mid V_\theta \mid \psi_{0\theta} \rangle , \tag{3.21}$$

where

$$b_{n'} = \sum_{i,n} \langle A_\theta \mid \Phi_n \rangle a_{in} (z-E_{i\theta})^{-1} a_{in'} . \tag{3.22}$$

A sequence of partial sums may be formed by successively taking the sum in Eq. (3.21) up to $j=0,1,\ldots,N-1$.

From these partial sums, one may then employ the epsilon algorithm to form the Padé tables.[43] In the case of the operator $G(z-H_0)$, we write Eq. (3.20) as

$$\langle A \mid \psi \rangle \cong \sum_{n''=0}^{N-1} c_{n''} \langle \Phi_{n''} \mid \psi_{0\theta} \rangle \ , \tag{3.23}$$

where

$$c_{n''} = \sum_{i,i',n,n'} \langle A_\theta \mid \Phi_n \rangle a_{in} (z - E_{i\theta})^{-1} a_{in'} \times a^{(0)}_{i'n'} (z - E^{(0)}_{i'\theta}) a^{(0)}_{i'n''} \ . \tag{3.24}$$

The sequence of partial sums is now obtained from the sum in Eq. (3.23). It may be noted that there are other places in these equations where Padé approximants might be formed from intermediate sums, but the procedures just described seem to give the best results.

IV. APPLICATION: SHORT-RANGE POTENTIAL

A. Matrix elements

The first example treated is the exponential potential,[2,57]

$$V(r) = -V_0 e^{-r/a} \ . \tag{4.1}$$

This was chosen since the $l=0$ problem may be solved exactly. The two Jost solutions are

$$f_\pm(k,r) = (\rho/2)^{\pm\nu} \Gamma(1 \mp \nu) J_{\pm\nu}(\rho x) \to e^{\pm ikr} \quad \text{as } r \to \infty \ , \tag{4.2}$$

where

$$\rho = 2a(2V_0)^{1/2} \ , \tag{4.3}$$

$$\nu = 2iak \ , \tag{4.4}$$

and

$$x = e^{-r/2a} \ . \tag{4.5}$$

The physical solution is therefore

$$\psi(k,r) = -\frac{1}{2i}[f_- - S(k) f_+] \to -\frac{1}{2i}[e^{-ikr} - S(k) e^{ikr}] \quad \text{as } r \to \infty \ , \tag{4.6}$$

where the S-matrix element has been defined in Eq. (2.10) in terms of the Jost functions,

$$F_\pm(k) = f_\pm(k,0) = (\rho/2)^{\pm\nu} \Gamma(1 \mp \nu) J_{\pm\nu}(\rho) \ . \tag{4.7}$$

In the Appendix a fairly general proof was given of Eqs. (2.27)–(2.30), the results of applying $1+GV$ and $i\epsilon G$ to the Jost solutions instead of the physical wave function. The current example has given us an opportunity to verify these equations analytically in a special case. The demonstration, which is only of passing interest, is not presented here.

Of more practical importance is the presence of an independent means of calculating the overlap of some L^2 function and the irregular or regular wave functions. For concreteness, we have taken the function $A(r)$ in Sec. III to be simply the $n=0$ Laguerre function in Eq. (3.12), but with a scale factor μ that may in general differ from the factor λ belonging to the basis used for diagonalization of the Hamiltonian. This L^2 function is typical of that which would be encountered in calculating a hydrogenic photoionization amplitude, requires only overlaps which are simple to evaluate, and provides (through the free parameter μ) some extra freedom in checking results. Using this choice of A and expanding the Bessel function in Eq. (4.2),

$$f_\pm(k,r) = x^{\mp\nu} \sum_{j=0}^{\infty} \left[-\frac{\rho^2 x^2}{4} \right]^j \Big/ j!(1 \mp \nu)_j = e^{\pm ikr} \sum_{j=0}^{\infty} \frac{(-2a^2 V_0 e^{-r/a})^j}{j!(1 \mp 2iak)_j} \ , \tag{4.8}$$

we get

$$\langle \Phi_0 \mid f_\pm \rangle = a^2 (\mu^3/2)^{1/2} \sum_{j=0}^{\infty} \frac{(-2a^2 V_0)^j}{j!(\mp 2iak)_j \left[\frac{a\mu}{2} \mp iak + j \right]^2} \ . \tag{4.9}$$

This series converges quite quickly, as does the series for the Jost function. Here $(c)_j = \Gamma(c+j)/\Gamma(c)$ is the Pochhammer symbol. With these two quantities, we can then compute

$$\langle \Phi_0 \mid (1+GV) \mid f_{0+} \rangle = \langle \Phi_0 \mid f_+ \rangle / F_+ \ , \tag{4.10}$$

$$\langle \Phi_0 \mid (1+GV) \mid f_{0-} \rangle = \langle \Phi_0 \mid f_+ \rangle / F_- - 2i \langle \Phi_0 \mid \psi \rangle \ , \tag{4.11}$$

and

$$\langle \Phi_0 \mid (1+GV) \mid \psi_0 \rangle = \langle \Phi_0 \mid \psi \rangle = \frac{f_-}{2i} \left[\frac{\langle \Phi_0 \mid f_+ \rangle}{F_+} - \frac{\langle \Phi_0 \mid f_- \rangle}{F_-} \right] . \tag{4.12}$$

This gives us a standard by which to judge the complex coordinate calculations.

There are several matrix elements which are needed for the numerical work, all of them including the complex quantity $\exp(i\theta)$. The first is the overlap between the Laguerre functions of order 2 and scale factor λ and the first Ricatti-Hankel functions:

$$\langle \Phi_n \mid \hat{h}^{(1)}_{0\theta} \rangle = \left[\frac{n!\lambda}{(n+2)!} \right]^{1/2} e^{i\theta/2} \int_0^\infty dr\, (\lambda r) L_n^2(\lambda r) e^{-\lambda r/2} e^{ikre^{i\theta}} = \left[\frac{n!}{\lambda(n+2)!} \right]^{1/2} e^{3i\theta/2} [1 - (n+2)(-q)^{n+1} + (n+1)(-q)^{n+2}] \ , \tag{4.13}$$

where

$$q=\frac{1+i\zeta}{1-i\zeta} \tag{4.14}$$

and

$$\zeta=2ke^{i\theta}/\lambda\ . \tag{4.15}$$

The integral for $\hat{h}^{(2)}_{0\theta}$ is obtained from Eq. (4.13) by the substitution $k\rightarrow -k$. We mention here that the corresponding integral for the Ricatti-Bessel function $\hat{j}_{0\theta}(kr)$ involves either Gegenbauer or Jacobi polynomials of complex argument. By far the most stable means of computing the latter integrals is to take linear combinations of the results for the Hankel functions. The second integral, used for the $1+GV$ wave operator, merely has an extra factor of the potential thrown in:

$$\langle\Phi_n\,|\,V_\theta\,|\,\hat{h}^{(1)}_{0\theta}\rangle=-V_0\left[\frac{n!}{\lambda(n+2)!}\right]^{1/2}e^{3i\theta/2}[1-(n+2)(-t)^{n+1}+(n+1)(-t)^{n+2}]\ , \tag{4.16}$$

where

$$t=\frac{1-\delta+i\zeta}{1+\delta-i\zeta}\ , \tag{4.17}$$

$$\delta=2e^{i\theta}/a\lambda\ . \tag{4.18}$$

The two remaining matrix elements come from the Hamiltonian and are very simple. The kinetic energy operator $H_{0\theta}$ is, for general l,

$$\langle\Phi_n\,|\,H_{0\theta}\,|\,\Phi_m\rangle=\lambda^2e^{-2i\theta}\times\begin{cases}\left[\dfrac{n!(m+2l+2)!}{m!(n+2l+2)!}\right]^{1/2}\dfrac{2m+2l+3}{2(2l+3)}\ , & m<n\\ \dfrac{4n+2l+3}{8(2l+3)}\ , & m=n\end{cases} \tag{4.19}$$

and the potential is

$$\langle\Phi_n\,|\,V_\theta\,|\,\Phi_m\rangle=-V_0\frac{(n+m+2)!}{[n!(n+2)!m!(m+2)!]^{1/2}}\frac{\delta^{n+m}}{(1+\delta)^{n+m+3}}\ {}_2F_1(-n,-m;-n-m-2;1-1/\delta^2)\ . \tag{4.20}$$

Hypergeometric transformations can be used to convert the Gauss function into other forms as convenience dictates. With this, we turn to a discussion of the numerical findings.

B. Numerical results

The results of the computations are very encouraging, even though the short-range potential does not provide as

TABLE I. Comparison of calculated versus exact amplitudes $\langle\Phi_0\,|\,\Omega\,|\,Z\rangle$ for the short-range potential $V=-V_0e^{-r/a}$. Here $\Phi_0=(\mu/2)^{1/2}\,\mu re^{-\mu r/2}$, $\Omega=1+GV$ or $G(z-H_0)$, and $Z=f_{0\pm}$ or ψ_0, the free-particle functions. The parameters chosen were $\mu=1$, $\lambda=2$, $\theta=20°$, $V_0=1$, $a=1$, and $k=1$.

	$N=10$	$N=20$	$N=30$	Exact
$\langle\Phi_0\,\|\,(1+GV)\,\|\,f_{0+}\rangle$[a]	−0.516 80	0.516 836 619	−0.516 836 642 19	−0.516 836 642 21
	+ 0.079 81i	+ 0.079 767 137i	+ 0.079 767 110 02i	+ 0.079 767 110 00i
$\langle\Phi_0\,\|\,(1+GV)\,\|\,f_{0-}\rangle$[a]	−0.431 50	−0.431 559 519	−0.431 559 433 60	−0.431 559 433 63
	−0.006 45i	−0.006 413 195i	−0.006 413 170 47i	−0.006 413 170 44i
$\langle\Phi_0\,\|\,(1+GV)\,\|\,\psi_0\rangle$[a]	0.043 13	0.043 090 166	0.043 090 140 25	0.043 090 140 222
	+ 0.042 65i	+ 0.042 638 600i	+ 0.042 638 604 29i	+ 0.042 638 604 292i
$\langle\Phi_0\,\|\,G(z-H_0)\,\|\,f_{0+}\rangle$[b]	−0.516 7	−0.516 836 576	−0.516 836 641 3	
	+ 0.079 7i	+ 0.079 767 266i	+ 0.079 767 107 7i	
$\langle\Phi_0\,\|\,G(z-H_0)\,\|\,f_{0-}\rangle$[b]	−0.431 3	−0.431 558 3	−0.431 559 433	
	−0.006 8i	−0.006 413 6i	−0.006 413 174i	
$\langle\Phi_0\,\|\,G(z-H_0)\,\|\,\psi_0\rangle$[b]	0.042 98	0.043 090 6	0.043 090 141	
	+ 0.042 68i	+ 0.042 638 9i	+ 0.042 638 605i	

[a]Computed directly.
[b]Computed with aid of Padé approximants.

TABLE II. First three columns of the Padé tables for each of the short-range $G(z-H_0)$ amplitudes in Table I. The approximants are denoted by $[L/M]$, where L is the degree of the numerator and M is that of the denominator. The first column ($M=0$) of each table contains the partial sums S_L from Eq. (4.22). Note the convergence of the $M=1,2$ columns in contrast to $M=0$ in the amplitudes for f_{0-} and ψ_0. The columns of the ψ_0 table are illustrated graphically in Fig. 1.

$\langle\Phi_0 \mid G(z-H_0) \mid f_{0+}\rangle$			$\langle\Phi_0 \mid G(z-H_0) \mid f_{0-}\rangle$			$\langle\Phi_0 \mid G(z-H_0) \mid \psi_0\rangle$		
−0.1002			0.2045			0.5928		
+ 0.3900i			−0.7955i			+ 0.1523i		
−0.5768	−0.4989		−1.2926	−0.5343		−0.0127	0.0883	
+ 0.2153i	+ 0.0885i		+ 0.2406i	+ 0.0881i		−0.3579i	+ 0.0247i	
−0.5386	−0.5257	−0.5182	−0.0729	−0.3784	−0.4324	−0.1289	0.0521	0.0502
+ 0.0691i	+ 0.0739i	+ 0.0752i	+ 0.3269i	+ 0.0431i	+ 0.0100i	+ 0.2328i	+ 0.0876i	+ 0.0477i
−0.5252	−0.5027	−0.5190	−0.2649	−0.4337	−0.4350	0.1649	0.0040	0.0447
+ 0.0727i	+ 0.0612i	+ 0.0786i	−0.2552i	+ 0.0554i	−0.0094i	+ 0.1302i	+ 0.0440i	+ 0.0461i
−0.5156	−0.5193	−0.5178	−0.6937	−0.4624	−0.4330	0.0563	0.0533	0.0428
+ 0.0728i	+ 0.0776i	+ 0.0802i	−0.0397i	−0.0336i	−0.0101i	−0.0890i	+ 0.0262i	+ 0.0424i
−0.5154	−0.5167	−0.5167	−0.3497	−0.4006	−0.4310	−0.0135	0.0422	0.0421
+ 0.0803i	+ 0.0796i	+ 0.0799i	+ 0.1072i	−0.0039i	−0.0055i	+ 0.0828i	+ 0.0575i	+ 0.0428i
−0.5169	−0.5167	−0.5167	−0.3724	−0.4405	−0.4309	0.0629	0.0274	0.0433
+ 0.0798i	+ 0.0799i	+ 0.0798i	−0.0459i	+ 0.0253i	−0.0071i	+ 0.0722i	+ 0.0383i	+ 0.0428i
−0.5166	−0.5167	−0.5168	−0.4964	−0.4421	−0.4312	0.0555	0.0483	0.0432
+ 0.0799i	+ 0.0798i	+ 0.0798i	−0.0311i	−0.0167i	−0.0066i	+ 0.0101i	+ 0.0373i	+ 0.0428i
−0.5166	−0.5168		−0.4168	−0.4176		0.0317	0.0416	
+ 0.0798i	+ 0.0798i		+ 0.0164i	−0.0034i		+ 0.0500i	+ 0.0496i	
−0.5168			−0.4133			0.0425		
+ 0.0798i			−0.0053i			+ 0.0517i		

stringent a test of the methods as the long-range example of the next section. In Table I, the amplitudes obtained for basis sizes $N=10$, 20, and 30 are compared with the exact values. It is evident that both forms of the wave operator, acting on any of the three particle wave functions, $f_{0\pm}$ or ψ_0, yield excellently convergent results.

There is a distinction, however, in the means used to extract these numbers for the two different operators. For $1+GV$, when Padé approximants were formed along the lines of Eqs. (3.21) and (3.22) from the partial sums

$$S_j=\sum_{n'=0}^{j} b_{n'}\langle\Phi_{n'} \mid V_\theta \mid Z_\theta\rangle\ ,\quad j=0,1,\ldots,N-1 \tag{4.21}$$

with $Z_\theta(k,r)$ a rotated version of any of $f_{0\pm}$ and ψ_0, it was found that the approximants were neither necessary nor of any help in obtaining satisfactory convergence. Consequently, the numbers for $1+GV$ in Table I represent just the results of direct calculations.

The operator $G(z-H_0)$, on the other hand, unquestionably benefits by introduction of the approximants, which are formed as a sequence of extrapolants from the partial sums [cf. Eqs. (3.23) and (3.24)]

$$S_j=\sum_{n''=0}^{j} c_{n''}\langle\Phi_{n''} \mid Z_\theta\rangle\ ,\quad j=0,1,\ldots,N-1\ . \tag{4.22}$$

For $N=10$, the first three columns of the Padé tables corresponding to $f_{0\pm}$ and ψ_0 are shown in Table II. The S_j form the elements of the first column of each table.

The results for $G(z-H_0)f_{0+}$ are fairly straightforward. The sequence of S_j's always seems to converge by itself to the same amplitude as $(1+GV)f_{0\pm}$. For parameters other than those of Tables I and II, however, convergence is sometimes accelerated by the Padé procedure.

The amplitudes for $G(z-H_0)f_{0-}$, and $G(z-H_0)\psi_0$ behave in a much more striking manner. The S_j's in the first columns of Table II appear not to converge very well at all. It is apparent, however, that things settle down fairly well even by the second column ($M=1$) in both cases, and improve as one moves further to the right. In fact, the sequences of partial sums are slowly spiraling into the right answers. This is demonstrated for ψ_0 by the solid line in Fig. 1(a). The convergence of the second and third column is demonstrated by the successive magnifications in Figs. 1(b) and 1(c).

For further contrast, Fig. 2 shows the behavior of the amplitude for $G(z-H_0)\psi_0$ for another choice of the parameters. Here the partial sums S_j spiral *outward*, as is also the case (not shown) for $G(z-H_0)f_{0-}$. It was not necessary to investigate these different circumstances in detail since the approximants converge in any case. We mention though, that the choice of parameters used in Fig. 2 did cause the $G(z-H_0)f_{0\pm}$ amplitudes to slip a bit in accuracy compared to that for $G(z-H_0)\psi_0$.

Thus, as opposed to the numbers in Table I for $1+GV$, those for $G(z-H_0)$ have been gleaned from the Padé tables using a criterion of relative agreement between neighboring approximants. (The last figure given is always uncertain.) It is clear that overall uniform reliability and ease favor the use of $1+GV$, but it is an interesting piece of information that two such disparate methods are

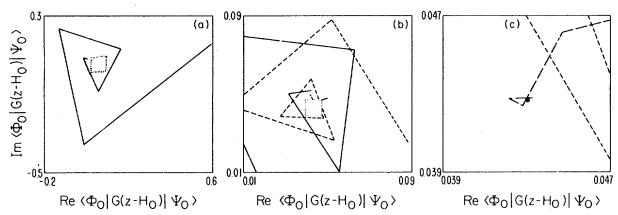

FIG. 1. Sequence of tenfold magnifications from (a) to (c) demonstrating the behavior of the columns of the $N=10$ Padé table in Table II for $\langle\Phi_0|G(z-H_0)|\psi_0\rangle$ with the short-range exponential potential of Eq. (4.1). Each line connects the series of $[L/M]$ approximants for a fixed M ($M=0$, solid curve; $M=1$, short-dash curve; $M=2$, long-dash curve). Although the partial sums (solid line) are spiraling in to the correct answer [dot in (c)], the approximants accelerate the convergence. Parameters used are $\mu=1$, $\lambda=2$, $\theta=20°$, $V_0=1$, $a=1$, and $k=1$.

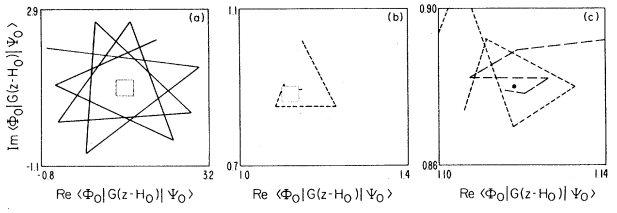

FIG. 2. Same as Fig. 1 except that the parameters are now $\mu=2$, $\lambda=1.5$, $\theta=25°$, $V_0=2$, $a=0.5$, and $k=0.5$. For this choice of parameters, the partial sums are spiraling outwards, but the approximants converge to the correct answer [the dot in (c)] anyway.

both aiming at the same answers. For the amplitudes employing ψ_0, both methods even seem to be of comparable quality.

One final point should not be overlooked. The procedures here are quite insensitive to variations in λ and θ over wide ranges. Thus it was not necessary to do any careful optimizations for these in the calculations.

V. APPLICATION: LONG-RANGE POTENTIAL

A. Matrix elements

As mentioned earlier, the methods employed here are applicable to long-range as well as short-range potentials. For the long-range example it was desired to model a polarization potential with r^{-4} behavior near infinity. To fit within our purview, it is necessary that this behavior be softened somewhat near the origin, and so the potential

$$V(r)=V_0(e^{-\gamma r}-1)^3/r^4 \rightarrow \begin{cases} -V_0/r^4 & \text{as } r\rightarrow\infty \\ -V_0\gamma^3/r & \text{as } r\rightarrow 0 \end{cases} \tag{5.1}$$

was chosen. We shall thus be investigating a potential which is not only long range, but also has a Coulombic singularity at the origin. In this case we have worked strictly with $l=1$.

The matrix elements for the overlap of the Laguerre functions of order 4 and the $l=1$ Hankel function are

$$\begin{aligned}\langle\Phi_n|\hat{h}^{(1)}_{1\theta}\rangle=\left[\frac{n!}{\lambda(n+4)!}\right]^{1/2} e^{i\theta/2}\frac{1-i\zeta}{4i\zeta}\{&2i\zeta[2(n+1)+2(n+4)q+(n+3)(n+4)(-q)^{n+2}\\&-2(n+1)(n+4)(-q)^{n+3}+(n+1)(n+2)(-q)^{n+4}]\\&-(1-i\zeta)[(n+1)(n+2)+2(n+1)(n+4)q\\&+(n+3)(n+4)q^2-2(n+4)(-q)^{n+3}+2(n+1)(-q)^{n+4}]\},\end{aligned} \tag{5.2}$$

where ζ and q have been defined in Eqs. (4.14) and (4.15). When the potential is sandwiched in between, things become considerably more difficult. The final result is

$$\langle\Phi_n|V_\theta|\hat{h}^{(1)}_{1\theta}\rangle=\left[\frac{n!\lambda^7}{(n+4)!}\right]^{1/2} V_0 e^{-7i\theta/2}\sum_{j=0}^{n}\frac{(-1)^j}{j!}\binom{n+4}{n-j}\left[K_{j+1}-\frac{2}{i\zeta}K_j\right], \tag{5.3}$$

where the quantities K_j are defined by

$$K_j=\frac{(-2)^{j-2}}{(2-j)!}\sum_{k=0}^{3}(-1)^k\binom{3}{k}(1+k\delta-i\zeta)^{2-j}\ln(1+k\delta-i\zeta),\quad 0\le j\le 2 \tag{5.4}$$

and

$$K_j=(j-3)!\sum_{k=0}^{3}(-1)^{k+1}\begin{bmatrix}3\\k\end{bmatrix}\left[\frac{2}{1+k\delta-i\xi}\right]^{j-2},\qquad j\geq 3\ . \tag{5.5}$$

The parameter δ is given by

$$\delta=2\gamma e^{i\theta}/\lambda\ . \tag{5.6}$$

The relevant potential elements are

$$\langle\Phi_n\mid V_\theta\mid\Phi_m\rangle=V_0\lambda^4 e^{-4i\theta}\left[\frac{n!m!}{(n+4)!(m+4)!}\right]^{1/2}\times\sum_{j=0}^{3}(-1)^{j+3}\begin{bmatrix}3\\j\end{bmatrix}V_{n,m}^{j}\ , \tag{5.7}$$

where

$$V_{n,m}^{j}=\begin{bmatrix}n+4\\4\end{bmatrix}\sum_{k=0}^{m}\begin{bmatrix}m+4\\m-k\end{bmatrix}\frac{(-1)^k}{(1+j\delta/2)^{k+1}}\times{}_2F_1\left[-n,k+1;5;\frac{1}{1+j\delta/2}\right]. \tag{5.8}$$

Since this problem is not exactly solvable, other means of checking the results are needed. It is evident from Eq. (2.11) that, for a real L^2 function, the argument of the total matrix element is simply the phase shift, and this can be obtained independently by numerical integration. This provides one criterion for judging the quality of the amplitude calculation.

A second test on the consistency of the results essentially employs the method used by Rescigno and McKoy[7] for computing photoionization cross sections. If we take the "elastic" matrix element of the Green's function in Eq. (2.23) between functions $A(r)$ and $A(r')$,

$$\langle A\mid G\mid A\rangle=-\frac{1}{ik}S(k)\left[\int_0^\infty dr\,A(r)f_+(k,r)\right]^2+\frac{1}{ik}\int_0^\infty dr\int_0^r dr'A(r)f_+(k,r)A(r')f_-(k,r')+\frac{1}{ik}\int_0^\infty dr\int_r^\infty dr'A(r)f_-(k,r)A(r')f_+(k,r')\ , \tag{5.9}$$

then it is evident that, for k and A real, the imaginary part of this matrix element is simply proportional to the square of the overlap of A and the physical wave function ψ:

$$\begin{aligned}\langle A\mid \mathrm{Im}G\mid A\rangle&=\frac{1}{2k}\left[\frac{F_-}{F_+}\left[\int_0^\infty dr\,A(r)f_+(k,r)\right]^2+\frac{F_+}{F_-}\left[\int_0^\infty dr\,A(r)f_-(k,r)\right]^2\right.\\&\qquad\left.-2\int_0^\infty dr\,A(r)f_+(k,r)\int_0^\infty dr'A(r')f_-(k,r')\right]\\&=[2kS(k)]^{-1}\left[\int_0^\infty dr\,A(r)[f_-(k,r)-S(k)f_+(k,r)]\right]^2\\&=(-1)^{l+1}\frac{2}{kS(k)}\left[\int_0^\infty dr\,A(r)\psi(k,r)\right]^2.\end{aligned} \tag{5.10}$$

Thus, taking A to be Φ_0, we can compute the ratio

$$\beta=\frac{2}{k}\frac{|\langle\Phi_0\mid\Omega\mid\psi_0\rangle|^2}{|\langle\Phi_0\mid\mathrm{Im}G\mid\Phi_0\rangle|}\ , \tag{5.11}$$

where both the numerator and denominator are obtained from the same finite basis calculation, and the numerator can be based on either the $1+GV$ or $G(z-H_0)$ methods. The smaller the quantity $\beta-1$, the better is the consistency.

It should be pointed out that there is already known one context in which complex coordinates may be applied to long-range potentials. Rescigno and Reinhardt[58] have shown that the Fredholm determinant, which is the same quantity as the Jost function J_+ in Eq. (2.6), can be obtained approximately through the numerical eigenvalues of H_θ and $H_{0\theta}$ in an N-term basis

$$J_+=\det\left[\frac{z-H_\theta}{z-H_{0\theta}}\right]\cong\prod_{i=1}^{N}\left[\frac{z-E_{i\theta}}{z-E_{i\theta}^{(0)}}\right]. \tag{5.12}$$

Thus the phase shift may be had from this sort of calculation as well. Values computed from the Fredholm method are included in the next section for comparison.

B. Numerical results

Some typical data from a convergence study for the long-range potential are shown in Table III. As for the case of the short-range potential, the Padé approximants are necessary for the success of the $G(z-H_0)$ method. What is new here, however, is that the convergence for $1+GV$ without the approximants is slower than with them, and so *all* of the amplitudes in the table have been extracted from the Padé tables. For purposes of comparison, we have also included the computed values of the ratio β in Eq. (5.11), and of the sine of the phase shift δ_1 [see Eq. (2.11)]. The exact value given for $\sin\delta_1$ was obtained by numerical integration. The values given for

$\sin\delta_{1F}$ were obtained by the determinantal Fredholm method in Eq. (5.12), and clearly do not compete with the present calculations.

As was to be expected, the results in general are not as well converged as in the short-range case, with the possible exception of $1+GV$ operating on f_{0+}. That the operator $1+GV$ should be the best behaved is in accord with the point made earlier that this involves less intermediate sums, and was already demonstrated for the exponential potential. The fact that the amplitude for $(1+GV)f_{0+}$ has more significant figures than $(1+GV)\psi_0$ at $N=30$ is evidence that, at least for the stability of the approximants, use of only the decreasing exponential can become a significant factor when the potential is long range. With smaller basis sizes (which do not reach as far out into the region where $f_{0\theta+}\cong 0$), we have noticed that $(1+GV)\psi_0$ can be more stable than $(1+GV)f_{0+}$. For instance, Figs. 3–5 show the convergence of the $N=10$ approximants for f_{0+}, f_{0-}, and ψ_0, respectively. Interestingly enough, the partial sums for $f_{0\pm}$ are spiraling inwards 180° out of phase, and the series in Figs. 3 and 4 are almost exact rotations of each other. When the two functions are combined to yield ψ_0, the resulting partial sums converge more quickly.

Note that $G(z-H_0)f_{0+}$ also fares somewhat better at higher N than $G(z-H_0)f_{0-}$, even though these amplitudes are both much worse than their $1+GV$ analogs. What is perhaps most curious is that, acting on the physical free-particle function, ψ_0, both forms of the wave operator remain competitive in terms of overall accuracy. The Padé tables for $G(z-H_0)\psi_0$ are much better behaved than those for $G(z-H_0)f_{0\pm}$. We can draw a tentative inference from this that $G(z-H_0)$ is much more sensitive to the Coulombic singularity of the potential at the origin. Very poor results are obtained with either of the functions which behave as $1/r$ at the origin, but the physical function ψ_0 (with its r^2 behavior) yields excellent results.

VI. DISCUSSION

The wave operator formalism has been shown to yield, with the aid of coordinate rotation, finite basis expansions, and Padé techniques, a method for computing overlaps between L^2 and continuum wave functions. This should be regarded as a first step toward the ultimate goal of calculating (total and partial) photoionization amplitudes in atomic and molecular systems. For the latter problem, however, one in general needs to tackle the full complexities of Coulomb scattering, and the next logical step is to attempt the computation of the hydrogenic photoeffect amplitude via Coulomb wave operators.

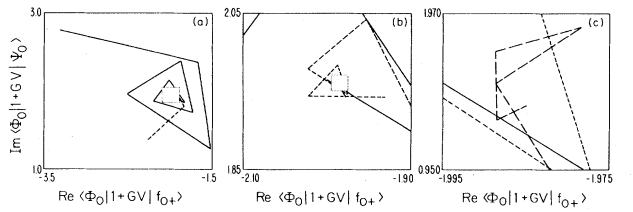

FIG. 3. Series of tenfold magnifications demonstrating the first three columns of the $N=10$ Padé table for $\langle\Phi_0|(1+GV)|f_{0-}\rangle$ with the long-range potential of Eq. (5.1). The Padé columns ($M=0$, solid curve; $M=1$, short-dash curve; $M=2$, long-dash curve) are all converging, although the partial sums (solid line) spiral inward rather slowly. Parameters used are $\mu=3$, $\lambda=3$, $\theta=25°$, $V_0=1$, $\gamma=1$, and $k=1$.

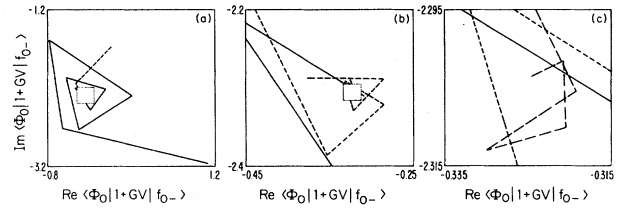

FIG. 4. Analog of Fig. 3 for the amplitude $\langle\Phi_0|(1+GV)|f_{0+}\rangle$. These two sequences are almost 180° rotations of each other.

The integrals considered here extend only over finite regions of space, a fact which allows us to consider long-range as well as short-range potentials. It should be noted, though, that familiar scattering information is calculated in the form of the phase shift. Furthermore, the methods were shown to be capable of much greater accuracy than the direct evaluation of the Fredholm determinant, the only other application to date of complex coordinates to problems involving long-range potentials.

For the scattering potentials considered above, approaches based on two different forms of the wave operator, $1+GV$ and $G(z-H_0)$, were shown to yield the same results. The $1+GV$ form seems to be preferable, however, since it involves fewer computational steps and appears to give greater accuracy.

Application of the wave operators to the individual Ricatti-Hankel functions has also been investigated, both theoretically and numerically. Theoretically, it was found that $1+GV$ operating on either Hankel function produces simple results in terms of the Jost solutions to the full Schrödinger equation, and these results were confirmed in the computations. One potentially useful point comes from the consistently good stability of calculations with f_{0+}, the Jost solution which damps when r is scaled by $\exp(i\theta)$. Equations (2.11) and (2.29) show that the physical wave function can be expressed in terms of $(1+GV)f_{0+}$:

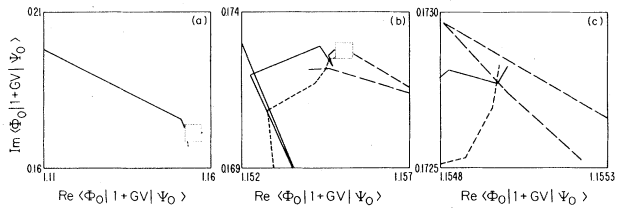

FIG. 5. Analog of Figs. 3 and 4 for the amplitudes $\langle\Phi_0|(1+GV)|\psi_0\rangle$. Convergence is seen to be much more rapid for this size of basis ($N=10$) than for either of the amplitudes involving $f_{0\pm}$.

TABLE III. Convergence study of amplitudes $\langle\Phi_0|\Omega|Z\rangle$ for the long-range potential $V=-V_0(e^{-\gamma r}-1)^3/r^4$. Here $\Phi_0=(\mu/24)^{1/2}(\mu r)^2e^{-\mu r/2}$, $\Omega=1+GV$ or $G(z-H_0)$, and $Z=f_{0\pm}$ or ψ_0. The parameters chosen were $\mu=3$, $\lambda=3$, $\theta=25°$, $V_0=1$, $\gamma=1$, and $k=1$. All matrix elements were extracted from Padé tables, with the exception of the quickly convergent $\langle\Phi_0|G|\Phi_0\rangle$, which is used in calculating the ratio β of Eq. (5.11). The quantity of the amplitudes can be judged by rates of convergence, the closeness of β to its theoretical value of 1, and agreement of the phase shift obtained from the ψ_0 amplitudes with the exact value obtained from numerical integration. For illustration, the phase shifts δ_{1F} obtained via the Fredholm method [Eq. (5.12)] are included.

	$N=10$	$N=20$	$N=30$
$\langle\Phi_0\|G\|\Phi_0\rangle$	0.080 154	0.080 310 817 67	0.080 310 834 5
	$-2.729\,041i$	$-2.728\,786\,230\,28i$	$-2.728\,786\,304\,8i$
$\langle\Phi_0\|(1+GV)\|f_{0+}\rangle$	$-1.984\,3$	$-1.984\,182\,4$	$-1.984\,182\,789\,7$
	$+1.960\,8i$	$+1.959\,726\,1i$	$+1.959\,728\,532i$
$\langle\Phi_0\|(1+GV)\|f_{0-}\rangle$	$-0.324\,5$	$-0.326\,143$	$-0.326\,186$
	$-2.305\,9i$	$-2.305\,763i$	$-2.305\,785i$
$\langle\Phi_0\|(1+GV)\|\psi_0\rangle$	1.155 23	1.155 179	1.155 184 5
	$+0.172\,90i$	$+0.173\,022i$	$+0.173\,029\,0i$
β	0.999 949	0.999 986 8	0.999 997 9
Exact: 1			
$\sin\delta_1$	0.148 02	0.148 127	0.148 132 2
Exact: 0.148 132 9(6)			
$\langle\Phi_0\|G(z-H_0)\|f_{0+}\rangle$	-1.90	$-1.956\,1$	$-1.970\,86$
	$+1.93i$	$+1.952\,1i$	$+1.954\,4i$
$\langle\Phi_0\|G(z-H_0)\|f_{0-}\rangle$	-0.46	-0.368	-0.352
	$-2.26i$	$-2.282i$	$-2.303i$
$\langle\Phi_0\|G(z-H_0)\|\psi_0\rangle$	1.155 18	1.155 177	1.155 184
	$+0.172\,64i$	$+0.173\,001i$	$+0.173\,026i$
β	0.999 798	0.999 978 1	0.999 996 3
$\sin\delta_1$	0.147 81	0.148 110	0.148 130
$\sin\delta_{1F}$	0.117	0.124	0.127

$$\psi=J_-\mathrm{Im}(i^{-l}f_+/J_+)$$
$$=J_-\mathrm{Im}[i^{-l}(1+GV)f_{0+}]\,. \tag{6.1}$$

Thus, providing that there is some independent means of calculating the Jost function (Fredholm determinant) accurately, overlaps involving the physical wave function may be obtained working strictly with f_{0+}.

ACKNOWLEDGMENTS

We would like to thank Professor John R. Taylor for helpful discussions and Dr. Karl F. Scheibner for discussions as well as invaluable computational assistance. This research was supported by National Science Foundation Grants Nos. CHE80-11442 and PHY82-00805. One of us (W. P. R.) acknowledges the hospitality and support of the National Bureau of Standards, Washington, D.C., during his tenure as a Visiting Scientist, 1982–83.

APPENDIX: $1+GV$ vs $i\epsilon G$

The proofs given here of Eqs. (2.24), (2.27), and (2.28) rest on the explicit form for the Green's function provided in Eq. (2.23). We first rewrite the functions in Eq. (2.24) as ($\epsilon\to0$ is implicit, and therefore so is $K\to k$)

$$\psi^{(1,2)}(k,r)=i\epsilon\mathrm{P}\int_0^\infty dr'G(K;r,r')f_{0\pm}(k,r')\,, \tag{A1}$$

where the principal value sign P indicates that the point $r'=r$ has been excluded. This is justified by using the continuity of G at $r'=r$:

$$G(K;r,r-0)=G(K;r,r+0)\,. \tag{A2}$$

Next, by virtue of Eqs. (2.20), (2.23), and the fact that the point $r'=r$ has been excluded from the integration, we may write

$$\psi^{(1,2)}=\mathrm{P}\int_0^\infty dr'f_{0\pm}(k,r')(H-\tfrac{1}{2}k^2)G(K;r,r')\,. \tag{A3}$$

The derivatives in H_0 may be integrated by parts to bring this operator over to $f_{0\pm}$, which obey Eqs. (2.3). We have

$$\mathrm{P}\int_0^\infty dr'f_{0\pm}\frac{d^2}{dr'^2}G=\mathrm{P}\int_0^\infty dr'G\frac{d^2}{dr'^2}f_{0\pm}+\left[\frac{dG}{dr'}f_{0\pm}\right]_0^{r-0}+\left[\frac{dG}{dr'}f_{0\pm}\right]_{r+0}^{\infty}$$
$$-\left[G\frac{df_{0\pm}}{dr'}\right]_0^{r-0}-\left[G\frac{df_{0\pm}}{dr'}\right]_{r+0}^{\infty}\,. \tag{A4}$$

The last two terms may be condensed by use of Eq. (A2). The first two terms in large parentheses may be condensed if we are careful to account for the discontinuity of G at $r=r'$,

$$\frac{d}{dr'}G(K;r,r+0)-\frac{d}{dr'}G(K;r,r-0)=2\ . \tag{A5}$$

Thus

$$\mathrm{P}\int_0^\infty dr'\frac{d^2G}{dr'^2}f_{0\pm}=\int_0^\infty dr'G\frac{d^2f_{0\pm}}{dr'^2}-2f_{0\pm}(K,r)+\left[\frac{dG}{dr'}f_{0\pm}\right]_0^\infty-\left[G\frac{df_{0\pm}}{dr'}\right]_0^\infty, \tag{A6}$$

where the P has been dropped from the integral on the right-hand side since no derivatives of G are involved. The surface terms can be further simplified by using the fact from Eqs. (2.4), (2.20), and (2.23) that both G and dG/dr' vanish at $r'=\infty$, and so this limit in the large parentheses contributes nothing. By virtue of Eqs. (2.7), (2.9), (2.12), and (2.17), we have the following small-r' limits:

$$f_{0\pm}(k,r')\to(2l-1)!!/(\mp ikr')^l\ , \tag{A7}$$

$$\frac{d}{dr'}f_{0\pm}(k,r')\to-\frac{l}{r'}(2l-1)!!/(\mp ikr')^l\ , \tag{A8}$$

$$G(K;r,r')\to-\frac{2}{F_+(K)}f_+(K,r)(r')^{l+1}\ , \tag{A9}$$

and

$$\frac{d}{dr'}G(K;r,r')\to-\frac{2(l+1)}{F_+(K)}f_+(K,r)(r')^l\ , \tag{A10}$$

leading to

$$\left[\frac{dG}{dr'}f_{0\pm}\right]_0^\infty-\left[G\frac{df_{0\pm}}{dr'}\right]_0^\infty=\lim_{r'\to0}\left[G\frac{df_{0\pm}}{dr'}-\frac{dG}{dr'}f_{0\pm}\right]=2i^{-l\pm l}f_+(K,r)/J_+(K)\ . \tag{A11}$$

Plugging this back into Eq. (A6), we obtain

$$\mathrm{P}\int_0^\infty dr'\frac{d^2G}{dr'^2}f_{0\pm}=\int_0^\infty dr'G\frac{d^2f_{0\pm}}{dr'^2}-2f_{0\pm}(k,r)+2i^{-l\pm l}f_+(K,r)/J_+(K)\ , \tag{A12}$$

which may be substituted in turn into Eq. (A1) to yield

$$\psi^{(1,2)}=i\epsilon Gf_{0\pm}=(1+GV)f_{0\pm}-i^{-l\pm l}f_+(k,r)/J_+(k)\ . \tag{A13}$$

Thus the Hankel functions obey an inhomogeneous version of Eq. (2.18); $i\epsilon G$ and $1+GV$ do not yield equivalent results when operating on them. The inhomogeneous term arises solely because the Hankel functions behave as r^{-l} at the origin, which is just sufficient to give the surface term in Eq. (A11) a finite value. Note that this term is a solution of the full Schrödinger equation, and that it too behaves in the same way as $f_{0\pm}$ near the origin:

$$i^{-l\pm l}f_+(k,r)/J_+(k)\to(2l-1)!!/(\pm ikr)^l \quad \text{as } r\to0\ . \tag{A14}$$

Equation (A13) is not the end of the story. It is also possible to show that $\psi^{(1)}$ is identically zero, and so only one of the Hankel functions contributes when the $i\epsilon G$ form of the wave operator is used. The proof of this is briefly sketched here for the $l=0$ case. Higher l is obviously more complicated.

To start, the explicit form of G given in Eq. (2.23) is used again in evaluating the functions $\psi^{(1,2)}$:

$$\psi^{(1,2)}(k,r)=i\epsilon\int_0^\infty dr'G(K;r,r')f_{0\pm}(k,r')=-\frac{2i\epsilon}{J_+(K)}\left[f_+(K,r)\int_0^r dr'\phi(K,r')e^{\pm ikr'}+\phi(K,r)\int_r^\infty dr'f_+(K,r')e^{\mp ikr'}\right]\ . \tag{A15}$$

The integral from 0 to r is nonsingular in any event, and so only the second integral is of concern:

$$\psi^{(1,2)}=-\frac{2i\epsilon}{K}\psi(K,r)\int_r^\infty dr'f_+(K,r')e^{\pm ikr'}\ . \tag{A16}$$

The best way to evaluate this is to use the integral equation satisfied by the irregular function,

$$f_+(K,r')=e^{iKr}-\frac{2}{K}\int_{r'}^\infty dr''\sin[K(r'-r'')]V(r'')f_+(K,r'')\ , \tag{A17}$$

where the first term on the right-hand side is called the Born term. With this,

$$\int_r^\infty dr'f_+(K,r')e^{\pm ikr'}=-\frac{e^{i(K\pm k)r}}{i(K\pm k)}-\frac{1}{iK}\int_r^\infty dr''V(r'')f_+(K,r'')\left[e^{-iKr''}\frac{e^{i(K\pm k)r}}{i(K\pm k)}-e^{iKr''}\frac{e^{i(-K\pm k)r'}}{i(-K\pm k)}\right]_{r'=r}^{r'=r''}\ . \tag{A18}$$

In the limit that ϵ goes to zero, these reduce to

$$\int_r^\infty dr' f_+(K,r')e^{ikr'} \to -\frac{e^{2ikr}}{2ik} - \frac{1}{ik}\int_r^\infty dr'' V(r'')f_+(k,r'')\left[\frac{e^{ikr''}-e^{2ikr-ikr''}}{2ik} - e^{ikr''}(r''-r')\right] \tag{A19}$$

and

$$\int_r^\infty dr' f_+(K,r')e^{-ikr'} \to -k/\epsilon - \frac{1}{ik}\int_0^\infty dr'' V(r'')f_+(k,r'')\left[e^{-ikr''}(r''-r) - \frac{e^{-ikr''}-e^{ikr''-2ikr}}{2ik}\right] . \tag{A20}$$

Thus, as long as the integrals in Eqs. (A17), (A19), and (A20) converge, only the factor $-k/\epsilon$ (stemming from the Born term) on the right-hand side of Eq. (A20) survives, and therefore Eq. (A16) becomes

$$\psi^{(1,2)}(k,r)=0 \tag{A21}$$

and

$$\psi^{(2)}(k,r)=-2i\psi(k,r) . \tag{A22}$$

This result, which for some reason does not appear to have found its way into the literature, is not completely restricted to the reasonable potentials mentioned above. For instance, Eq. (A21) is true for the Coulomb potential, as well. The Coulomb analog of Eq. (A22), however, entails a phase factor which is divergent as $\epsilon \to 0$.

Combining Eqs. (A13), (A21), and (A22), one obtains the results of $1+GV$ acting on the irregular functions, given above in Eqs. (2.29) and (2.30).

*Permanent address: Department of Chemistry, University of Colorado, Boulder, CO 80309 and Joint Institute for Laboratory Astrophysics, University of Colorado and National Bureau of Standards, Boulder, CO 80309.

[1]C. Møller, K. Dan. Vidensk. Selsk. Mat.-Fys. Medd. 23, 1 (1945); Reprinted in *Quantum Scattering Theory,* edited by M. H. Ross (Indiana University Press, Bloomington, 1963).
[2]R. G. Newton, *Scattering Theory of Waves and Particles* (McGraw-Hill, New York, 1966).
[3]J. R. Taylor, *Scattering Theory: The Quantum Theory of Nonrelativistic Collisions* (Wiley, New York, 1972).
[4]B. R. Junker, Adv. At. Mol. Phys. 18, 207 (1982).
[5]W. P. Reinhardt, Ann. Rev. Phys. Chem. 33, 223 (1982).
[6]W. P. Reinhardt, Comput. Phys. Commun. 17, 1 (1979).
[7]T. N. Rescigno and V. McKoy, Phys. Rev. A 12, 522 (1975).
[8]T. N. Rescigno, C. W. McCurdy, and V. McKoy, J. Chem. Phys. 64, 447 (1976).
[9]C. V. Sukumar and K. C. Kulander, J. Phys. B 11, 4155 (1978).
[10]S.-I. Chu and W. P. Reinhardt, Phys. Rev. Lett. 39, 1195 (1977).
[11]C. W. McCurdy, Phys. Rev. A 21, 464 (1980).
[12]C. W. McCurdy and T. N. Rescigno, Phys. Rev. A 21, 1499 (1980).
[13]V. E. Semenov, Opt. Spektrosk. 48, 723 (1980) [Opt. Spectrosc. (USSR) 48, 398 (1980)].
[14]A. Maquet, S.-I. Chu, and W. P. Reinhardt, Phys. Rev. A 27, 2946 (1983).
[15]C. Holt, M. G. Raymer, and W. P. Reinhardt, Phys. Rev. A 27, 2971 (1983).
[16]C. W. McCurdy and T. N. Rescigno, Phys. Rev. A 20, 2346 (1979).
[17]R. Yaris and H. S. Taylor, Chem. Phys. Lett. 66, 505 (1979).
[18]T. Noro and H. S. Taylor, J. Phys. B 13, L377 (1980).
[19]Z. Bačic and J. Simons, Int. J. Quant. Chem. 21, 727 (1981).
[20]J. Nuttall and H. L. Cohen, Phys. Rev. 188, 1542 (1969).
[21]F. A. McDonald and J. Nuttall, Phys. Rev. C 6, 121 (1972).
[22]J. A. Hendry, Nucl. Phys. 198A, 391 (1972).
[23]S. B. Raju and G. Doolen, Phys. Rev. A 9, 1965 (1974).
[24]R. T. Baumel, M. C. Crocker, and J. Nuttall, Phys. Rev. A 12, 486 (1975).
[25]B. R. Johnson and W. P. Reinhardt (unpublished).
[26]E. J. Heller, W. P. Reinhardt, and H. A. Yamani, J. Comput. Phys. 13, 536 (1973).
[27]E. J. Heller, T. N. Rescigno, and W. P. Reinhardt, Phys. Rev. A 8, 2946 (1973).
[28]H. A. Yamani and W. P. Reinhardt, Phys. Rev. A 11, 1144 (1975).
[29]P. W. Langhoff, C. T. Corcoran, J. S. Sims, F. Weinhold, and R. M. Glover, Phys. Rev. A 14, 1042 (1976).
[30]P. W. Langhoff, in *Electron-Molecule and Photon-Molecule Collisions,* edited by T. Rescigno, V. McKoy, and B. Schneider (Plenum, New York, 1979).
[31]S. V. ONeil and W. P. Reinhardt, J. Chem. Phys. 69, 2126 (1978).
[32]L. H. Beard and D. A. Micha, Chem. Phys. Lett. 53, 329 (1978).
[33]Z. C. Kuruoglu and D. A. Micha, J. Chem. Phys. 72, 3327 (1980).
[34]L. Schlessinger and C. Schwartz, Phys. Rev. Lett. 16, 1173 (1966).
[35]L. Schlessinger, Phys. Rev. 167, 1411 (1968).
[36]L. Schlessinger, Phys. Rev. 171, 1523 (1968).
[37]F. A. McDonald and J. Nuttall, Phys. Rev. Lett. 23, 361 (1969).
[38]F. A. McDonald and J. Nuttall, Phys. Rev. A 4, 1821 (1971).
[39]S. C. Pieper, L. Schlessinger, and J. Wright, Phys. Rev. D 1, 1674 (1970).
[40]S. C. Pieper, L. Schlessinger, and J. Wright, Phys. Rev. D 2, 1561 (1970).
[41]S. C. Pieper, L. Schlessinger, and J. Wright, Phys. Rev. D 3, 2419 (1971).
[42]G. Doolen, G. McCartor, F. A. McDonald, and J. Nuttall, Phys. Rev A 4, 108 (1971).
[43]J. Nuttall, in *Invited Papers and Progress Reports of the Seventh International Conference on the Physics of Electronic and Atomic Collisions, Amsterdam, 1971,* edited by P. R. Govers and F. G. de Heer (North-Holland, Amsterdam, 1972), p. 265.
[44]J. Nuttall, Comput. Phys. Commun. 6, 331 (1974).
[45]G. A. Baker, Jr., *Essentials of Padé Approximants* (Academic, New York, 1975).

[46]J. B. Donahue, P. A. M. Gram, M. V. Hynes, R. W. Hamm. C. A. Frost, H. C. Bryant, K. B. Butterfield, D. A. Clark, and W. W. Smith, Phys. Rev. Lett. 48, 1538 (1982).
[47]G. Wannier, Phys. Rev. 90, 817 (1953).
[48]H. Klar and W. Schlecht, J. Phys. B 9, 1699 (1976).
[49]C. Bottcher, J. Phys. B 15, L463 (1982).
[50]A. Temkin, Phys. Rev. Lett. 49, 365 (1982).
[51]C. H. Greene and A. R. P. Rau, Phys. Rev. Lett. 48, 533 (1982).
[52]P. Grujić, J. Phys. B 15, 1913 (1982).
[53]The theory of scattering for central potentials is sufficiently well known that we content ourselves with a few basic definitions that will be needed in later sections. The discussion is culled from Chap. 12 of Ref. 2. Only one value of the angular momentum l will be considered at a time, so this subscript on many of the operators and functions should be regarded as implicit.
[54]B. Simon, *Quantum Mechanics for Hamiltonians Defined as Quadratic Forms* (Princeton University Press, Princeton, N. J., 1971).
[55]Following the physicists' convention, $\psi(K,r)$ in Eq. (2.9) and $G(K;r,r')$ in Eq. (2.23) should be superscripted with a + sign (the retarded case). This is suppressed in order to avoid a proliferation of $\pm$ signs.
[56]It should be noted that the factors of $\exp(i\theta/2)$ in A_θ and $\psi_{0\theta}$ arise because the volume element is dr in this paper. With the normal r^2dr, they are factors of $\exp(3i\theta/2)$.
[57]R. K. Roychoudhury, J. Phys. A 13, 1137 (1980).
[58]T. N. Rescigno and W. P. Reinhardt, Phys. Rev. A 8, 2828 (1973).